

Effects of Foot-and-Mouth Disease Virus Nonstructural Proteins on the Structure and Function of the Early Secretory Pathway: 2BC but Not 3A Blocks Endoplasmic Reticulum-to-Golgi Transport

Katy Moffat,^{1†} Gareth Howell,^{1†} Caroline Knox,² Graham J. Belsham,¹ Paul Monaghan,¹ Martin D. Ryan,² and Thomas Wileman^{1*}

Pirbright Laboratory, BBSRC Institute for Animal Health, Pirbright, Surrey,¹ and School of Biology, Centre for Biomolecular Sciences, University of St. Andrews, North Haugh, St. Andrews,² United Kingdom

Received 12 July 2004/Accepted 23 November 2004

Infection of cells by picornaviruses leads to the generation of intracellular membrane vesicles. The expression of poliovirus (PV) 3A protein causes swelling of the endoplasmic reticulum (ER) and inhibition of protein trafficking between the ER and the Golgi apparatus. Here, we report that the nonstructural proteins of a second picornavirus, foot-and-mouth disease virus (FMDV), also perturb the secretory pathway. FMDV proteins 3A, 2B, 2C, and 2BC expressed alone in cells were recovered from crude membrane fractions, indicating membrane association. Immunofluorescence microscopy showed that 3A was located in a reticular structure and 2B was located in the ER, while 2C was located in both the ER and the bright punctate structures within the Golgi apparatus. 2BC gave punctate cytoplasmic staining and also caused accumulation of ER proteins in large vesicular structures located around the nuclei. The effect of the FMDV proteins on the trafficking of the vesicular stomatitis virus glycoprotein (G protein) from the ER to the cell surface was determined. Unlike its PV counterpart, the 3A protein of FMDV did not prevent trafficking of the G protein to the cell surface. Instead, surface expression of the G protein was blocked by 2BC, with retention of the G protein in a modified ER compartment staining for 2BC. The results suggest that the nonstructural proteins of different picornaviruses may vary in their ability to perturb the secretory pathway. Since FMDV 2BC can block the delivery of proteins to the cell surface, it may, as shown for PV 3A, play a role in immune evasion and contribute to the persistent infections observed in ruminants.

It has been known for several years that the secretory pathway is disrupted in cells infected with picornaviruses (3, 11, 13–15, 31, 38, 48). This is characterized by the appearance of large numbers of membrane vesicles in the cytoplasm. In the case of poliovirus (PV) infection, the membrane vesicles are thought to originate from the endoplasmic reticulum (ER), either from COPII-coated vesicles that move proteins from the ER to the Golgi apparatus or from double-membraned vacuoles that extend from the ER during autophagy (6, 37, 43). Several studies suggest that the rearranged membranes are utilized during virus replication (7, 10, 40, 43). Viral proteins responsible for replication and newly synthesized viral RNA are, for example, associated with these membranes, and membrane fractions isolated from infected cells can synthesize viral RNA *in vitro* (6, 44, 47). A link between a functioning secretory pathway and virus replication has also been provided by the observation that brefeldin A (BFA), a drug that blocks ER-to-Golgi transport by preventing the formation of transport vesicles, blocks replication of PV (23, 28). The membrane rearrangements seen within infected cells are caused by the nonstructural proteins encoded by the P2 and P3 regions of the genome. Studies on the activity of individual PV proteins and the membranes they modify have implicated a role for the

nonstructural proteins 3A, 2B, and 2BC. The PV 2C and 2BC proteins bind membranes and cause vesiculation and tubulation of the ER, and in some cases, this remodeling of the ER is extensive and results in myelin-like swirls of ER-derived membrane (1, 10, 46). Similarly, the PV 3AB protein has also been shown to induce membrane alterations, such as myelin-like whirls, to the ER (16). The PV 3A protein also binds membranes but induces swelling of ER membrane cisternae (14). Interestingly, the membrane rearrangements induced by individual proteins are often more extensive than those seen in infected cells, and recent studies show that coexpression of 3A with 2BC is required to produce vesicles morphologically similar to those seen at sites of PV replication (43).

In addition to providing the membranes required for picornavirus replication, the ER and Golgi apparatus are also important for the delivery of proteins to the surfaces of cells (33, 35, 39). This is particularly important in the context of a virus infection where secretion of cytokines and the cell surface expression of major histocompatibility complex (MHC) proteins loaded with viral peptides enable infected cells to be recognized by the innate and acquired immune system. The secretion of alpha and beta interferons, for example, induces major changes in gene expression within infected cells and cells surrounding the site of infection (8, 9). This leads to increased expression of antiviral proteins, for example, MX and PKR, which are thought to slow the replication of the virus. Many viral infections lead to the activation of NF- κ B, a transcription factor, which increases the expression and consequent secretion of several proinflammatory cytokines such as interleukin-1

* Corresponding author. Mailing address: Institute for Animal Health, Pirbright Laboratory, Ash Road, Pirbright, Surrey GU24 0NF, United Kingdom. Phone: 44 01483 232441. Fax: 44 01483 232448. E-mail: thomas.wileman@bbsrc.ac.uk.

† K.M. and G.H. contributed equally to this work.

(IL-1), IL-6, and tumor necrosis factor alpha (TNF- α) (25). These chemokines attract cells of the immune system to sites of infection and enhance their proliferation and differentiation. The secretory pathway also plays a key role in delivering MHC class 1 peptide complexes to the surfaces of cells for presentation to cytotoxic T cells, allowing the elimination of virus-infected cells (22). Interestingly, recent work has suggested that modulation of the host protein secretory pathway induced by PV 3A, affecting the movement of proteins through the secretory pathway, may offer an immunological advantage to the virus. The PV 3A protein has, for example, been shown to reduce the secretion of beta interferon, IL-6, and IL-8 and to compromise MHC class 1 antigen presentation (11, 13). The block in the secretory pathway may also increase cell survival since PV 3A has been shown to protect cells from TNF- α -induced apoptosis by reducing expression of the TNF receptor at the cell surface (31).

To date, most studies on the effects of picornavirus nonstructural proteins on membrane traffic and secretion have been carried out using PV proteins. There are differences between the nonstructural proteins encoded by different picornaviruses (see below). Hence, it is possible that the nonstructural proteins encoded by different picornaviruses may differ in their effects on the secretory pathway.

Foot-and-mouth disease virus (FMDV) is a picornavirus which causes an economically important disease of ruminants. The main barrier to the effective control of FMDV through vaccination is the establishment of persistent infections in infected and vaccinated animals. Live virus can be recovered from probang samples taken from the upper respiratory tracts of persistently infected animals, and these animals are therefore excluded from the food chain and eliminated by slaughter (2). The establishment of a persistent infection by FMDV suggests that the virus has a mechanism to inhibit innate and acquired immune defenses. Given the observations on the effect of PV infection on the integrity of the secretory pathway and the ability of PV 3A to block trafficking of interferons, cytokines, and MHC molecules, we have studied the effects of individual FMDV nonstructural proteins on the delivery of membrane proteins to the cell surface. The results show that, unlike PV 3A, the FMDV 3A protein does not block the secretory pathway; instead, ER-to-Golgi transport is inhibited by FMDV 2BC.

MATERIALS AND METHODS

Plasmids. The FMDV nonstructural proteins 2Bv5 (which contains a V5 C-terminal tag), 2BC, 2C, and 3A were expressed using the pcDNA 3.1 expression vector (Invitrogen, Paisley, United Kingdom). Vesicular stomatitis virus O45 temperature-sensitive glycoprotein (VSV TsO45 G) fused to cyan fluorescent protein (CFP) was the kind gift of Jennifer Lippincott-Schwartz (National Institutes of Health, Bethesda, Md.). To allow easier detection of the VSV TsO45 GCFP protein in immunofluorescence studies, the CFP sequence was changed to yellow fluorescence protein (YFP). The YFP sequence was generated from PCR of pEYFP-C1 (BD Biosciences, Oxford, United Kingdom) by using the primers 5'-CGC GGA TCC AAT GGT GAG CAA GGG CGA and 5'-AAG CGG CCG CGA ATT CAC TTG TAC AGC TCG TCC AT. A BamHI site was introduced upstream of the ATG start codon. EcoRI and NotI sites were introduced downstream of the stop codon. The BamHI-NotI fragment of YFP was inserted in place of the CFP sequence (pTsO45 GCFP) to make pTsO45 GYFP. pDsRed2-ER, which expresses a fusion protein consisting of *Discozyma* sp. red fluorescent protein with the ER targeting sequence of calreticulin fused to its N

terminus and the ER retention sequence KDEL fused to the C terminus, was used for fluorescent labeling of the ER within living cells (BD Biosciences).

Transfection of cells. Vero cells (ECACC 84113001; the European Collection of Cell Cultures, Wiltshire, United Kingdom) were grown to 70% confluency in 5% CO₂ at 37°C in HEPES-buffered Dulbecco modified Eagle's medium containing 10% fetal calf serum, 100 Système International units of penicillin/ml, 100 μ g of streptomycin/ml, and 20 mM L-glutamine. Cells were then transfected with plasmid DNA (0.5 μ g/well in a 24-well plate or 46 μ g/175-cm² flask) by using Transfast (Promega, Southampton, United Kingdom) in HEPES-buffered Dulbecco modified Eagle's medium for 1 h at 37°C.

Antibodies. Rabbit antibody N- β -COP was raised to the synthetic peptide CKKEAGELKPEEEITVGPVQK. Rabbit antibody TW20 was raised against a peptide representing the C terminus of calnexin. Rabbit anti-ERp57 has been described previously (36). Mouse anti-FMDV 2C (3F7) and mouse anti-FMDV 3A (2C2) were a kind gift of E. Brocchi (Istituto Zooprofilattico Sperimentale della Lombardia e dell'Emilia, Brescia, Italy). Rabbit antibody DM12 that recognizes FMDV 2C was provided by D. Mackay (Institute for Animal Health, Pirbright, Surrey, United Kingdom). Mouse anti-V5 was purchased from Invitrogen. A mouse monoclonal antibody (I1) recognizing the ectodomain of the VSV G protein was a generous gift from Douglas Lyles (Wake Forest University School of Medicine, Wake Forest, N.C.) and has been described previously (27).

Metabolic labeling and cellular fractionation. Vero cells grown to approximately 90% confluence in 175-cm² flasks were trypsinized and labeled metabolically for 2 h at 37°C by using 10 MBq of ³⁵S-Promix (Amersham Life Sciences, Little Chalfont, St. Giles, United Kingdom) per ml in methionine- and cysteine-free media. Washed cells were suspended in 8% (wt/vol) buffered sucrose (50 mM Tris, 1mM EDTA [pH7.4]) containing 1 μ g/ml each of leupeptin, pepstatin, chymostatin, and antipain (Roche, Lewes, United Kingdom) and homogenized by 20 passages through a 25-gauge syringe needle. Whole cells and nuclei were removed by centrifugation at 6,000 rpm for 2 min at 4°C in a Sorval Fresco centrifuge. Postnuclear supernatants were then spun at 13,000 rpm for 20 min at 4°C in the same machine. The resulting supernatant was buffered with 50 mM HEPES [pH7.4], and membrane (P) and cytosol (SN) fractions were separated by centrifugation at 33,000 rpm for 2 h at 4°C in a Beckman L8-M ultracentrifuge. The membrane pellet was dissolved in immunoprecipitation buffer (10 mM Tris [pH7.8]; 0.15 M NaCl; 10mM iodoacetamide; 1mM EDTA; 1mM phenylmethylsulfonyl fluoride; 1 μ g/ml each of leupeptin, pepstatin, chymostatin, and antipain [Roche] per ml; 2% [vol/vol] Triton X-100). In parallel experiments, the level of aggregated insoluble protein in the membrane fraction was determined by solubilizing the postnuclear membrane fraction in immunoprecipitation buffer prior to centrifugation. Insoluble aggregated protein was recovered in a pellet (P*) generated by centrifugation at 13,000 rpm for 20 min at 4°C in a Sorval Fresco centrifuge. The accompanying supernatant contained proteins extracted from the membrane (SN*). The aggregated proteins in the pellet were solubilized in 1% sodium dodecyl sulfate (SDS) in 50 mM HEPES [pH7.4] and diluted 100-fold in immunoprecipitation buffer. All fractions were immunoprecipitated using antibodies coupled to protein A and analyzed by SDS-polyacrylamide gel electrophoresis (PAGE) followed by autoradiography as described previously (36).

Indirect immunofluorescence and microscopy. Cells were seeded onto 13-mm-diameter glass coverslips (Agar Scientific, Stanstead, United Kingdom) and transfected in situ. Samples were fixed in 4% (wt/vol) paraformaldehyde in phosphate-buffered saline (PBS) for 45 min at room temperature, washed in PBS, and stored at 4°C. Cells were permeabilized and incubated in blocking buffer 1 (50 mM Tris [pH 7.4], 150 mM NaCl, 1% [wt/vol] gelatin, 1% [vol/vol] Nonidet P-40, 30% [vol/vol] normal goat serum) with shaking for 15 min at room temperature. Primary antibodies were diluted in blocking buffer 1 and incubated with coverslips for 30 min at room temperature. Samples were then washed three times in 0.5% Tween 20 (Sigma, Poole, United Kingdom) in PBS. Primary antibodies were detected with Alexa 488-, Alexa 568- or Alexa 633-conjugated species-specific immunoglobulins (Molecular Probes through Invitrogen) diluted 1:200 in blocking buffer 1. DNA was stained with 50 ng of DAPI (4',6'-diamidino-2-phenylindole; Sigma)/ml. Coverslips were mounted in Vectashield (Vector Laboratories, Peterborough, United Kingdom) and imaged in a Leica TCS SP2 confocal microscope.

For surface staining, cells were incubated in blocking buffer 2 (50 mM Tris [pH 7.4], 150 mM NaCl, 1% [wt/vol] gelatin, 30% [vol/vol] normal goat serum) with shaking for 15 min at room temperature. Primary antibodies were diluted in blocking buffer 2 and incubated with coverslips for 30 min at room temperature. Cells were then permeabilized and incubated in blocking buffer 1 by using the same procedure described above for further primary antibody incubations and then detection.

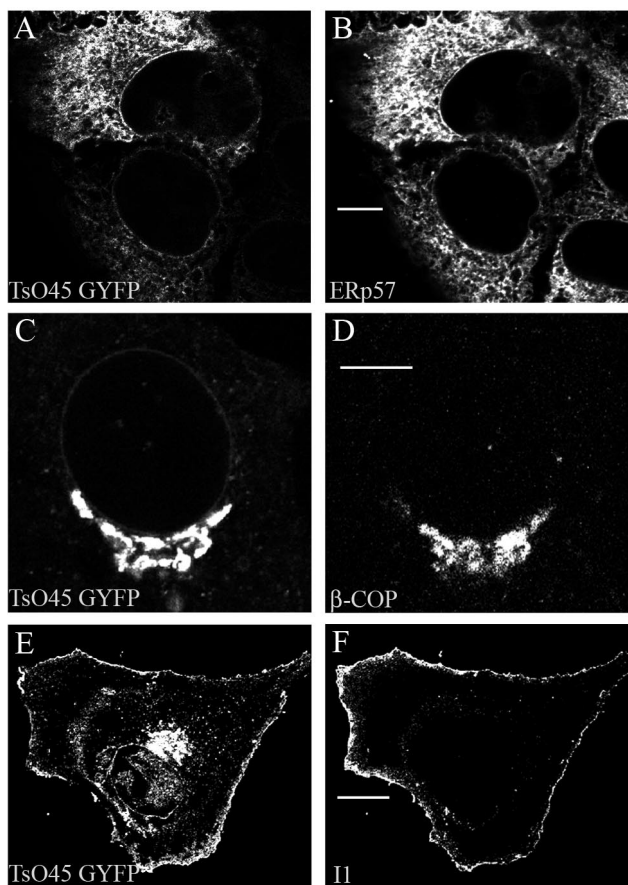


FIG. 1. Distribution of VSV TsO45 GYFP protein at permissive and nonpermissive temperatures. Vero cells expressing TsO45 GYFP were incubated for 48 h at 40°C (A and B). Cells were also incubated for a further 30 min (C and D) or 3 h (E and F) at 32°C. For intracellular staining (panels B and D), cells were fixed, permeabilized, and counterstained using antibodies specific for ERp57 or using β -COP as indicated in the panel. For surface staining (panel F), cells were incubated with an antibody (II) specific for the ectodomain of the G protein before permeabilization. Intracellular TsO45 GYFP (panels A, C, and E) was visualized through the natural fluorescence of YFP. Primary antibodies were detected using goat antibody conjugated to Alexa-568 (panels B, D, and F). Bars, 8 μ m (panels B and D) or 16 μ m (panel F).

RESULTS

The YFP-linked G protein of TsO45 VSV can be used to follow membrane transport through the secretory pathway to the plasma membrane. The G protein of the O45 temperature-sensitive mutant of VSV (TsO45 G) has been used extensively to study the transport of membrane proteins through the secretory pathway (5, 12, 21, 29, 34) and to study the effect of PV on membrane traffic (15). When cells expressing the TsO45 G protein are grown at 40°C, the protein misfolds and is retained in the ER. Lowering the temperature to 32°C allows the G protein to fold correctly, form a trimer, and move to the Golgi apparatus and from there to the cell surface (18, 26). Figure 1 shows cells expressing a TsO45 G fusion protein where YFP has been added to the cytoplasmic tail of the protein (TsO45 GYFP). In panel A, cells were grown at 40°C and the G protein was seen located in a reticular structure spread through

the cytoplasm of the cell that was suggestive of the ER. This was confirmed when TsO45 GYFP protein was shown to be colocalized with resident ER protein ERp57 (panel B). Figure 1C shows cells incubated at 40°C and then cooled to 32°C for 30 min. Under these conditions (shown at higher magnification), the G protein fluorescence was located in a crescent situated to one side of the nucleus, indicating transport to the Golgi apparatus, and the YFP signal colocalized with Golgi protein β -COP (panel D). In none of these images was cell surface staining for the G protein observed. To test for transport to the cell surface, cells were incubated at 32°C for a further 3 h. An antibody (II) recognizing the ectodomain of the G protein was added to cells prior to permeabilization; cells were then fixed and processed for immunofluorescence. In Fig. 1F, cell surface expression of the G protein is indicated by the bright staining at the plasma membrane produced by the monoclonal antibody. There was also a residual intracellular signal indicated by the perinuclear fluorescence signal from TsO45 GYFP remaining in the Golgi apparatus (Fig. 1E). In the experiments described below, this transport assay was used to test the effects of FMDV nonstructural proteins on the transport of the G protein from the ER to the Golgi apparatus and from there to the cell surface.

Comparison of amino acid sequences of picornavirus nonstructural proteins 2BC and 3A. Most studies on the effects of picornavirus nonstructural proteins on membrane traffic and secretion have been carried out using PV proteins. The sequence alignment in Fig. 2 shows, however, that there are significant differences between the nonstructural proteins encoded by different picornaviruses. Regions were aligned using the multiple alignment construction and analysis workbench (MACAW), and blocks of similarity were detected with a pairwise cutoff score of 25 (minimum of two sequences). Sequence similarities of 70 to 100% and 30 to 70% are shown. It is apparent that the 2C proteins of picornaviruses show high conservation; however, proteins 2B and 3A are quite different. The 3A proteins also show wide differences in length: rhinovirus 3A proteins are some 77 amino acids and enterovirus 3A proteins some 87 amino acids, while the aphthovirus FMDV 3A protein is much longer, with 153 amino acids. Given these differences, it is possible that the nonstructural proteins encoded by different picornaviruses may differ in their effects on the secretory pathway.

Effect of FMDV 3A on the secretory pathway. The PV 3A protein has been shown to associate with membranes and block the secretory pathway when expressed alone in cells. To see if FMDV 3A also binds membranes, the protein was expressed alone in cells and the presence of 3A in crude membrane fractions was tested by immunoprecipitation (Fig. 3). Cells expressing FMDV 3A were metabolically labeled for 2 h and then homogenized. Whole cells and nuclei were removed by low-speed centrifugation, and postnuclear membranes were pelleted, leaving a supernatant containing cytosolic proteins. Fractions were then dissolved in detergent prior to immunoprecipitation with an antibody specific for FMDV 3A. Control precipitations were carried out using antibodies specific for calnexin, an integral membrane protein of the ER. Figure 3A compares control and transfected cells, and the top panel shows that fractionation was successful since the signal for calnexin was recovered from the membrane fraction. In the

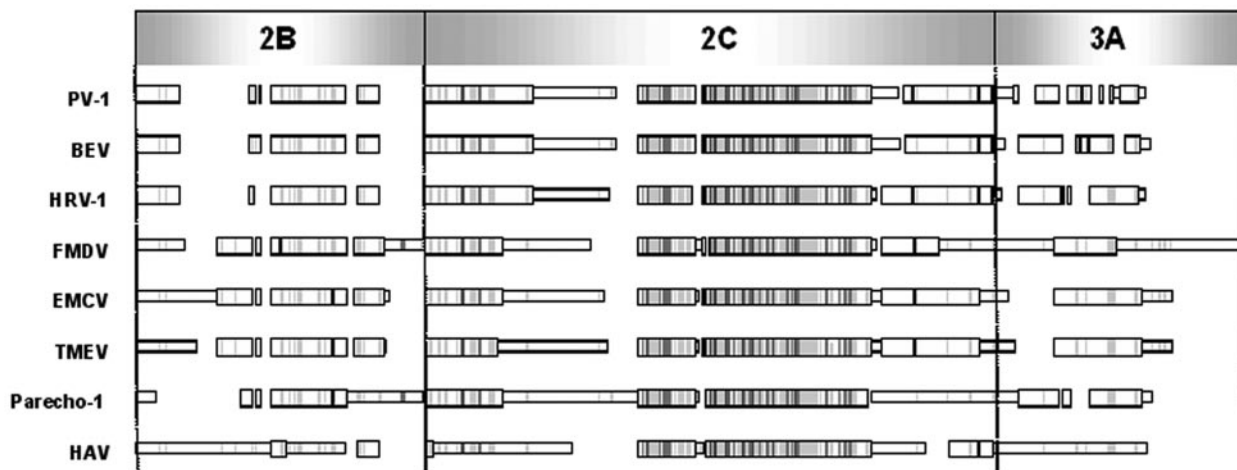


FIG. 2. Amino acid sequence comparison between the 2BC through 3A regions of picornaviruses. PV type 1, bovine enterovirus (BEV), human rhinovirus type 1 (HRV-1), FMDV, encephalomyocarditis virus (EMCV), Theiler's murine encephalitis virus (TMEV), and hepatitis A virus (HAV) 2B, 2C, and 3A regions were aligned using MACAW (41). Blocks of similarity were detected with a pairwise cutoff score of 25 (minimum of two sequences). Sequence similarities of 70 to 100% are shown by dark grey bars, while similarities of 30 to 70% are shown by light grey bars.

same experiment, approximately 50% of the cellular pool of FMDV 3A was recovered from the cytosolic protein fraction and the rest was recovered from the membrane fraction, suggesting some association of FMDV 3A with membranes in cells. In experiments of this kind, it is important to show that proteins are recovered in a membrane fraction because they are really associated with membranes and not because they cosediment because of insolubility and aggregation. This can be ruled out if the protein fails to pellet when membranes are dissolved in mild detergent before centrifugation (19). Comparison of the soluble membrane fraction and the insoluble aggregate fraction (SN* and P*, respectively) showed that when postnuclear membranes are solubilized prior to centrifugation, the FMDV 3A and calnexin are both recovered from the soluble membrane fraction (SN*). This suggests that 3A did not aggregate in cells.

The effect of 3A on the movement of membrane proteins from the ER into the secretory pathway was tested by following the TsO45 GYFP protein as described above. Cells cotransfected with vectors expressing FMDV 3A and the TsO45 GYFP protein were grown at 40°C for 48 h and then shifted to 32°C for 30 min or 3 h and analyzed by fluorescence microscopy (Fig. 3). At each time point, FMDV 3A was located throughout the cytoplasm and on a diffuse reticular structure (panels B, E, and H). This was in agreement with the membrane fractionation suggesting that 3A was both membrane associated and in the cytosol. The diffuse reticular staining for 3A is likely to be the ER and is consistent with earlier work showing the association of transiently expressed FMDV 3A with membranes containing calreticulin (32). Figure 3C shows the reticular distribution of TsO45 GYFP in cells grown at 40°C. Note there was no concentration of a perinuclear YFP signal indicative of the Golgi apparatus in these images, and the cells expressing TsO45 GYFP lacked surface expression of the G protein (panel D), demonstrating retention of the G protein in the ER at 40°C. Panels E to G show cells observed after 30 min at 32°C. The G protein had moved to the Golgi apparatus, but there was no cell surface expression of the G

protein (panel G). This was true in all cells, whether expression of FMDV 3A was detected or not, showing that 3A did not prevent ER-to-Golgi transport. Panels H to J show cells observed after 3 h at 32°C. FMDV 3A (Fig. 3H) remained associated with diffuse reticular structures. Significantly, all the cells, regardless of whether they were expressing 3A, showed strong staining for the G protein in the Golgi apparatus and at the plasma membrane (panels I and J). Taken together, these results show that FMDV 3A associates with cellular membranes but, unlike the PV 3A protein, does not prevent the ability of the secretory pathway to deliver TsO45 GYFP to the Golgi apparatus and from there to the cell surface.

Effect of FMDV P2 proteins on transport through the secretory pathway. The experiments described above suggested that FMDV 3A does not stop movement of membrane proteins from the ER to the cell surface. Similar experiments were therefore used to examine whether the P2 proteins encoded by FMDV affect the secretory pathway. Figure 4 shows the membrane fractionation of cells expressing FMDV 2B. The 2B protein migrated at approximately 17 kDa on SDS-PAGE gels and was immunoprecipitated from the membrane fraction and copartitioned with calnexin, indicating membrane association in cells. The immunoprecipitates of the cytosolic fraction included proteins of 18 and 15 kDa that were present in the untransfected control extracts; however, a protein of 17 kDa representative of 2B was absent from this fraction, showing that the 2B protein was predominantly membrane associated. Again, the possibility that the proteins pelleted because of aggregation was tested by solubilizing membranes in mild detergent before centrifugation. In each case, the proteins were recovered exclusively from the solubilized fraction (SN*), indicating a lack of protein aggregation.

The subcellular location of FMDV 2B expressed in cells was analyzed by fluorescence microscopy (Fig. 4B to G). At low levels of expression, the 2B protein was distributed within a reticular structure that spread throughout the cytoplasm, and at high levels, the protein accumulated as a honeycomb structure in the juxtannuclear area (results not shown). When the

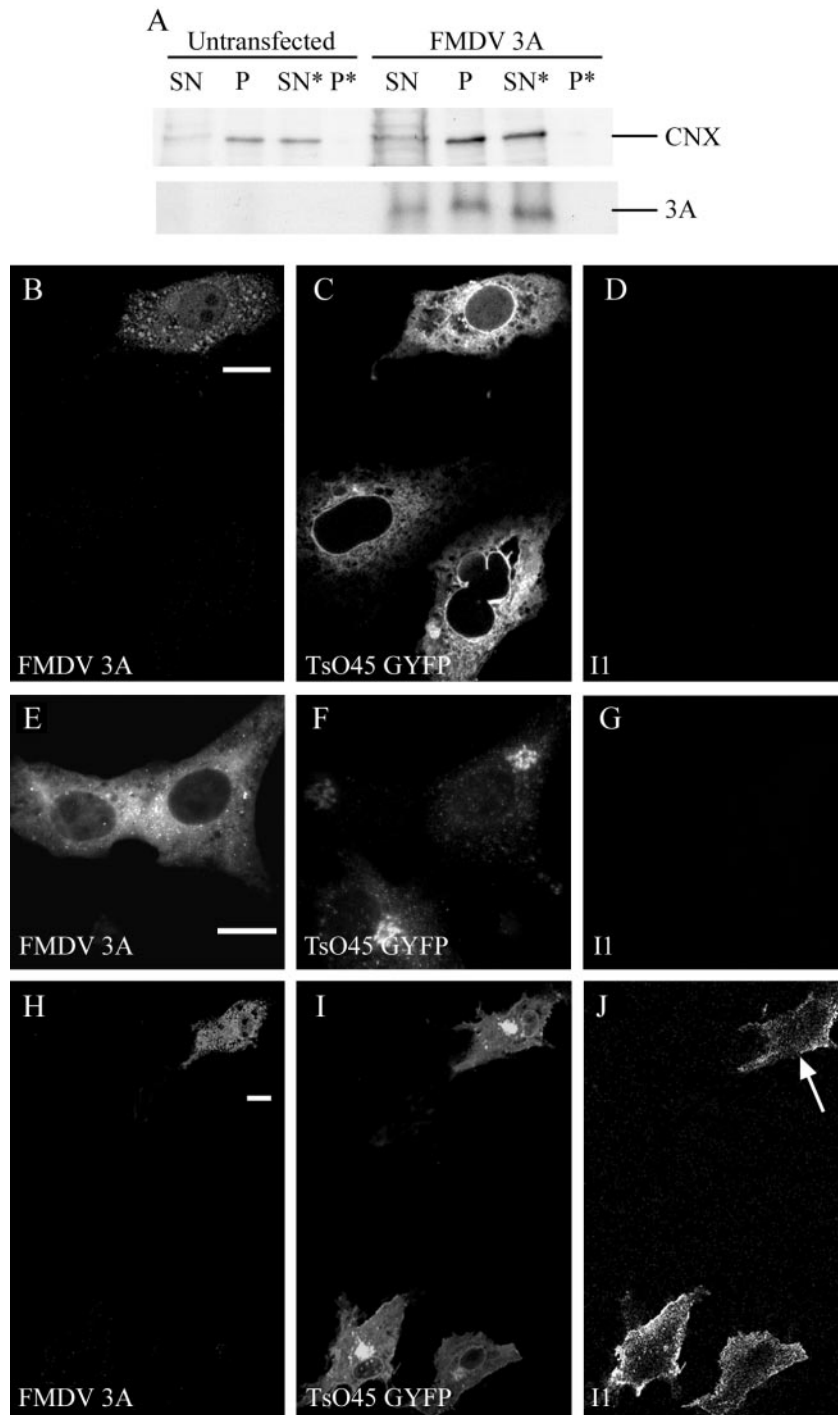


FIG. 3. FMDV 3A is membrane associated but does not block transport of VSV TsO45 GYFP protein to the cell surface. (A) Membrane association of FMDV protein 3A. Mock-transfected Vero cells or Vero cells expressing FMDV 3A were metabolically labeled with [³⁵S]methionine-cysteine and then homogenized. Postnuclear supernatants were separated by centrifugation into crude cytosol (SN) and membrane (P) fractions. Half the membrane fraction was solubilized in 2% Triton X-100 and recentrifuged to produce a solubilized membrane fraction (SN*) and a pellet of insoluble aggregated protein (P*). Equivalent fractions were immunoprecipitated using antibodies specific for 3A (2C2) or calnexin (CNX). Proteins were resolved by SDS-PAGE and detected by autoradiography. (B to J) Transport of VSV TsO45 GYFP protein to the surfaces of cells transfected with FMDV 3A. Vero cells were transiently cotransfected with plasmids which express TsO45 GYFP and FMDV 3A and incubated for 48 h at 40°C (panels B to D). A set of cells was also incubated for a further 30 min (panels E to G) or 3 h (panels H to J) at 32°C. All cells were fixed with 4% paraformaldehyde, and surface expression of the G protein was detected by adding an antibody (II), recognizing the ectodomain of the G protein, prior to permeabilization (panels D, G, and J). Cells were then permeabilized, and intracellular staining of FMDV 3A was visualized using antibody 2C2 (panels B, E, and H). Intracellular TsO45 GYFP was visualized directly using the signal from YFP (panels C, F, and I). Primary antibodies were visualized with appropriate goat antibodies conjugated to Alexa-568 (panels B, E, and H) or Alexa-633 (panels D, G, and J). Bars, 10 μm. Arrow indicates surface staining of G protein in cells expressing FMDV 3A.

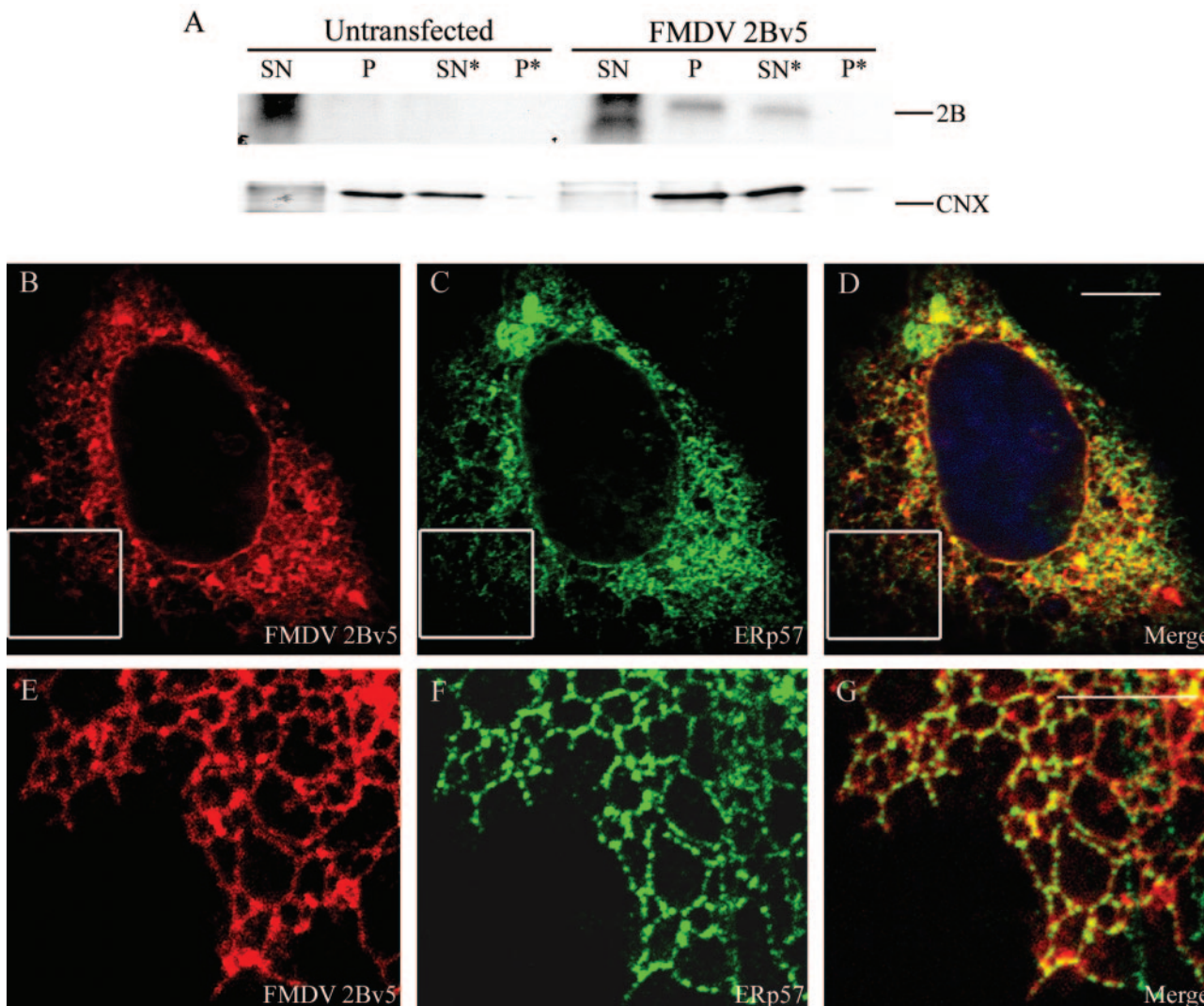


FIG. 4. Subcellular location of FMDV 2B. (A) Membrane association of FMDV protein 2B. Vero cells were mock transfected or transfected with a vector encoding 2Bv5. After 48 h, cells were fractionated as described in the legend to Fig. 3A. The V5-epitope-tagged 2B (2Bv5) was immunoprecipitated using antibody specific for the V5 tag (V5). Calnexin was detected using an anti-peptide antibody (CNX). Proteins were resolved by SDS-PAGE and detected by autoradiography. (B to G) Intracellular distribution of FMDV 2B. Vero cells expressing 2Bv5 were fixed in 4% paraformaldehyde and then permeabilized. 2Bv5 was detected using the epitope tag (panels B and E). Cells were counterstained using antibody specific for ERp57 (panels C and F). Primary antibodies were visualized with appropriate goat antibodies conjugated to Alexa-568 (panels A and E) or Alexa-488 (panels C and F). Panels D and G are digitally merged images. Panels E to G are higher magnifications of the insets defined in panels B to D, respectively. Bars, 8 μ m (panel D) or 4 μ m (panel G).

distribution of 2B was compared with that of ERp57, the fluorescence signals were closely aligned in reticular structures, suggesting an association of 2B with the ER. Similar studies were performed for 2BC and 2C (Fig. 5). The subcellular fractionation showed copartitioning of both proteins with calnexin (Fig. 5A), showing that they were membrane associated in cells. The subcellular distribution of 2BC and 2C within transfected cells was also examined by fluorescence microscopy. Staining for 2C produced a faint reticular pattern reminiscent of ER and bright punctate staining next to the nucleus (panels B and E). The faint reticular-like 2C stain colocalized with ERp57 (panel C), suggesting ER location. Interestingly, the bright juxtannuclear structures did not colocalize with ERp57 (panel D) and the juxtannuclear position of 2C sug-

gested some association with the Golgi apparatus. When cells were counterstained using antibodies specific for the Golgi protein β -COP, it was apparent that 2C was also found located in punctate clusters that stained strongly for β -COP (panels E to G). When merged, (panel G), it was apparent that there was incomplete overlap in the 2C and β -COP signals. These results suggested that FMDV 2C may also bind to Golgi elements, but as FMDV 2C did not colocalize with β COP, this may suggest that β COP is excluded from the location of 2C.

The distribution of FMDV 2BC within transfected cells was also examined and is shown in Fig. 5H to J. Surprisingly, the signal for 2BC did not resemble that of either 2B or 2C. FMDV 2BC was located in small punctate structures scattered throughout the cytoplasm. The protein was also located in

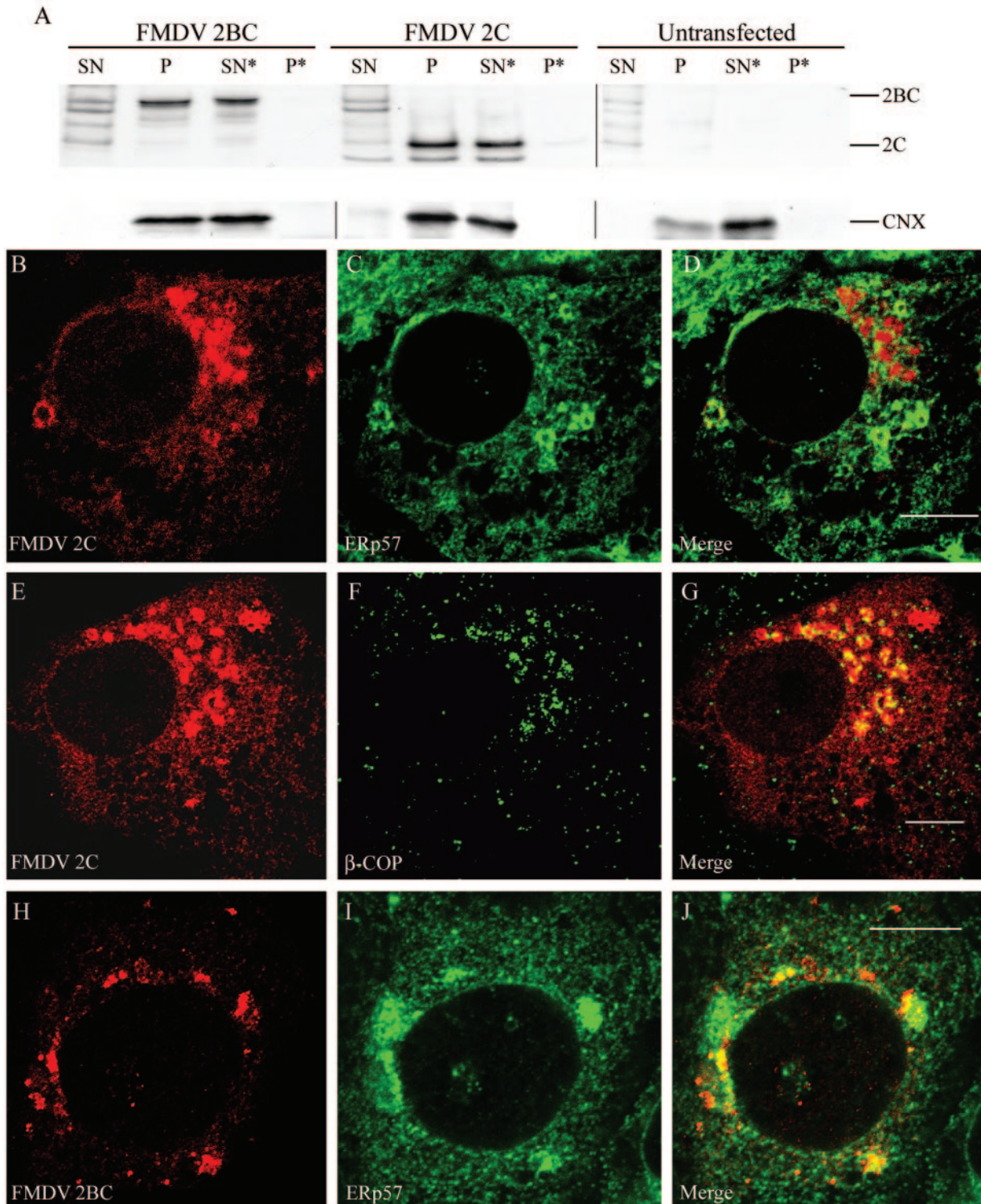


FIG. 5. Subcellular location of FMDV 2BC and 2C. (A) Membrane association of FMDV proteins 2BC and 2C. Vero cells were mock transfected or transfected with a vector encoding 2BC or 2C. After 48 h, cells were fractionated as described in the legend to Fig. 3A. Both 2C and 2BC were immunoprecipitated using the DM12 antibody specific for 2C. Calnexin was detected using an antipeptide antibody (CNX). Proteins were resolved by SDS-PAGE and detected by autoradiography. (B to J) Intracellular distribution of FMDV 2BC and 2C. Vero cells expressing 2C (panels B to G) or 2BC (panels H to J) were fixed in 4% paraformaldehyde and then permeabilized. 2C and 2BC were both detected using antibody 3F7 (panels B, E, and H), and cells were counterstained using antibodies against ERp57 (panels C and I) or β -COP (panel F). Primary antibodies were visualized with appropriate goat antibodies conjugated to Alexa-568 (panels B, E, and H) or Alexa-488 (panels C, F, and I). Panels D, G, and J are digitally merged images. Bars, 8 μ m.

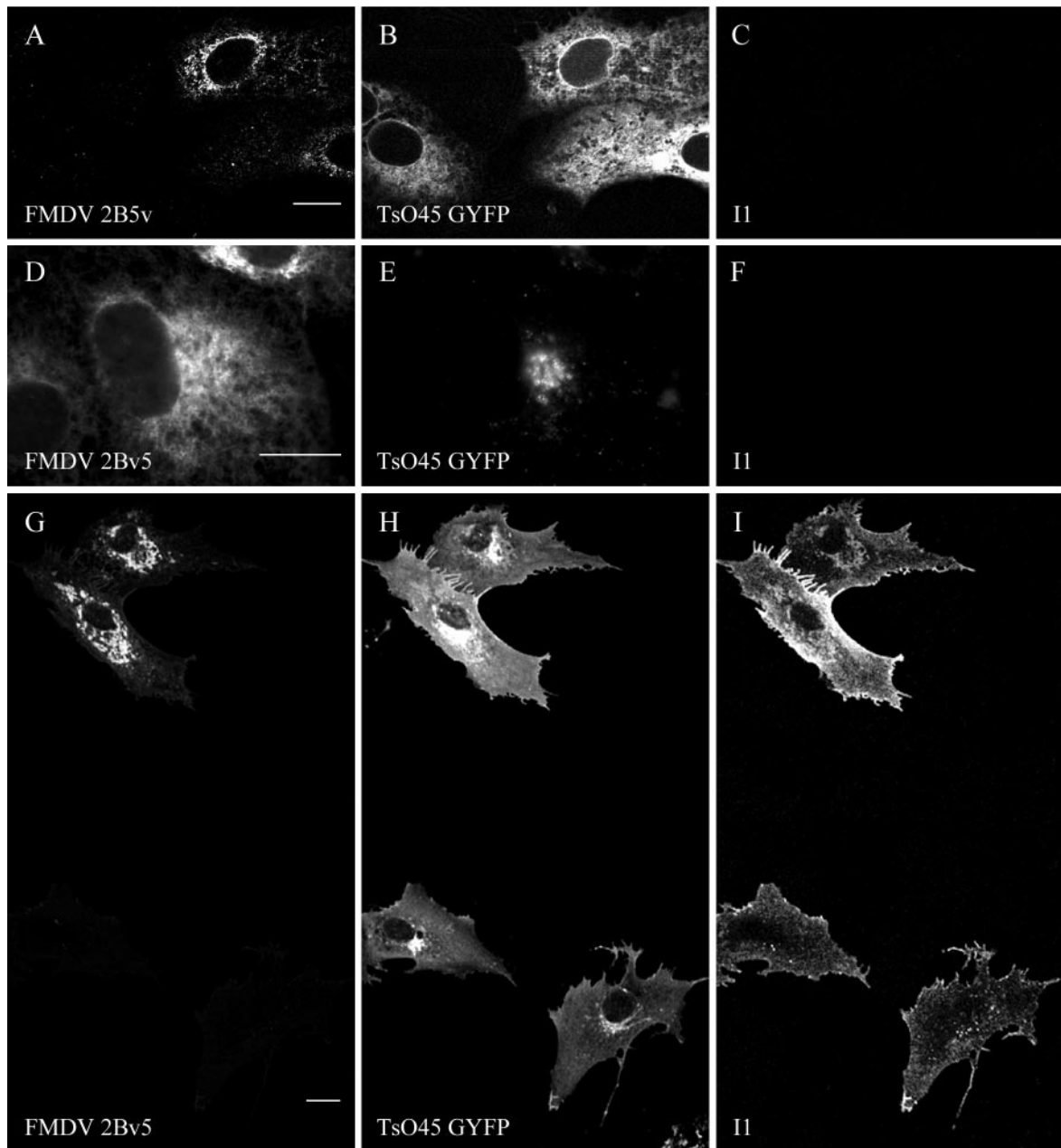


FIG. 6. FMDV 2B does not block transport of VSV TsO45 GYFP protein to the cell surface. Vero cells were transiently cotransfected with TsO45 GYFP and FMDV 2Bv5 and incubated for 48 h at 40°C (A to C). Some cells were also incubated for a further 30 min (D to F) or 3 h (G to I) at 32°C. All cells were fixed with 4% paraformaldehyde, and surface expression of the G protein was detected by adding an antibody (II), recognizing the ectodomain of the G protein, prior to permeabilization (panels C, F, and I). Cells were then permeabilized, and 2Bv5 was detected using the epitope tag (panels A, D, and G). Intracellular TsO45 GYFP was visualized directly using the signal from YFP (panels B, E, and H). Primary antibodies were visualized with appropriate goat antibodies conjugated to Alexa-568 (panels A, D, and G) or Alexa-633 (panels C, F, and I). Bars, 10 μ m.

larger structures surrounding the nucleus (panel H). Most interesting was the observation that expression of FMDV 2BC resulted in redistribution of the ER marker ERp57 (panel I) into brightly staining structures, many of which were also located around the nucleus. There were clearly large, bright structures that were positive for ERp57 but were negative for 2BC; however, these structures were always close to areas that accumulated FMDV 2BC.

The effects of individual P2 protein on the movement of the TsO45 GYFP protein from the ER to the cell surface was tested using the temperature shift experiment described above for FMDV 3A. Cells expressing P2 proteins and the TsO45 GYFP protein were maintained at 40°C for 48 h and then shifted to 32°C for 30 min or 3 h. Figure 6 shows cells expressing TsO45 GYFP and FMDV 2B. At 40°C, the G protein was located in a reticular structure suggestive of the ER (panel B)

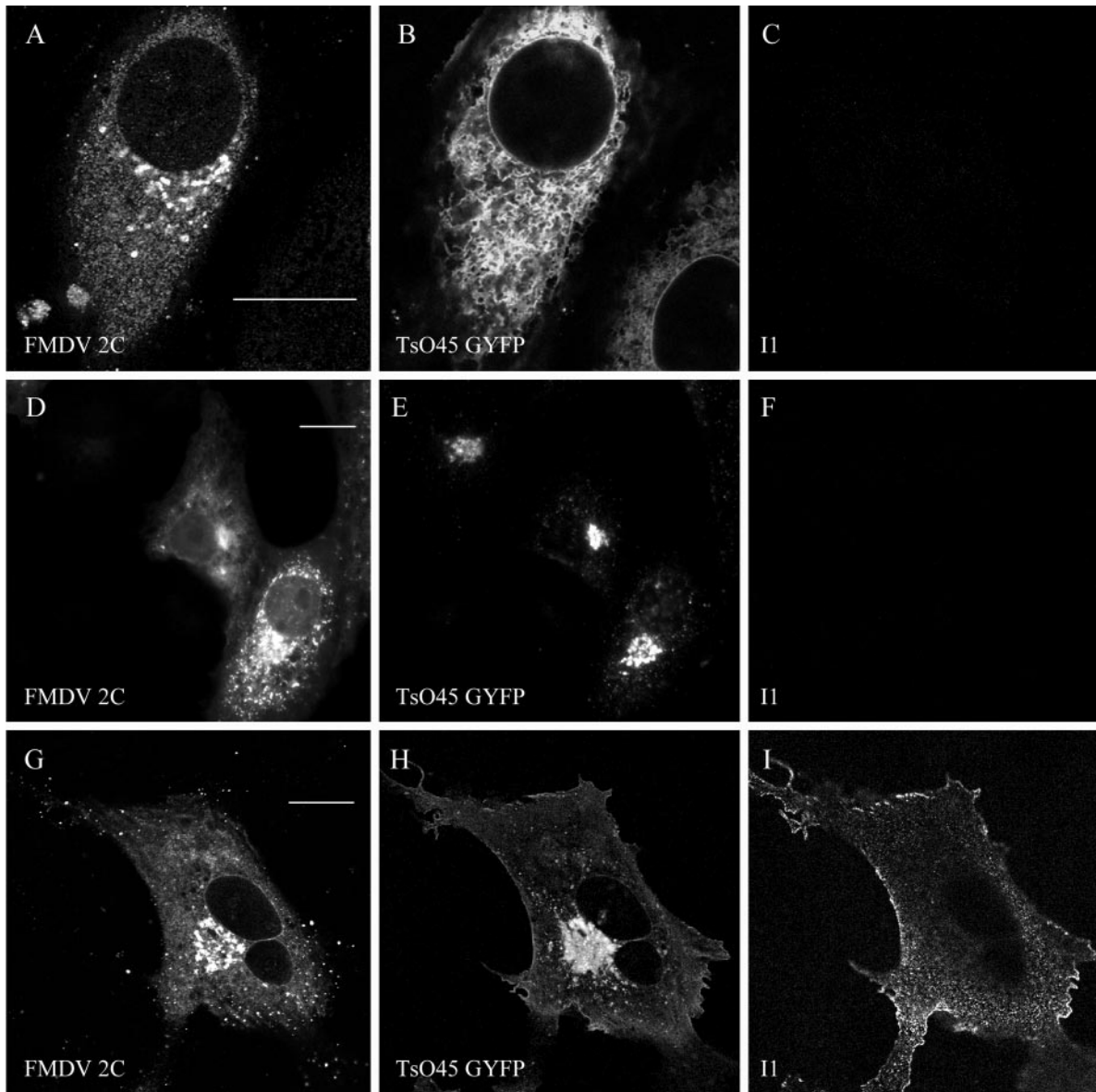


FIG. 7. FMDV 2C does not block transport of VSV TsO45 GYFP protein to the cell surface. Vero cells were transiently cotransfected with TsO45 GYFP and FMDV 2C and incubated for 48 h at 40°C (A to C). Some cells were also incubated for a further 30 min (D to F) or 3 h (G to I) at 32°C. All cells were fixed, and surface expression of the G protein was detected by adding an antibody (II), recognizing the ectodomain of the G protein, prior to permeabilization (panels C, F and I). Cells were then permeabilized, and 2C was detected using antibody 3F7 (panels A, D, and G). Intracellular TsO45 GYFP was visualized directly using the signal from YFP (panels B, E, and H). Primary antibodies were visualized with appropriate goat antibodies conjugated to Alexa-568 (panels A, D, and G) or Alexa-633 (panels C, F, and I). Bars, 10 μ m.

and was absent from the cell surface (panel C). At this non-permissive temperature, the FMDV 2B protein was located in a reticular structure (panel A) very similar to that of the G protein (panel B), suggesting they were separate from the ER. The temperature shift had little effect on the distribution of 2C, which remained in perinuclear clusters (panels D and G). Figure 7E shows that FMDV 2C did not prevent movement of the G protein to the Golgi apparatus at 30 min (panel E) or to the cell surface after 3 h (panel I). Panels G to I show cells observed 3 h after the temperature shift. The 2B protein remained reticular (panel G), but the TsO45 GYFP protein had now reached the surface in transfected cells (panels H and I). A similar experiment was performed for 2C (Fig. 7). The majority of FMDV 2C protein was in punctate structures in a

perinuclear Golgi-like location (panel A). These structures did not colocalize with the reticular signal from the G protein (panel B), suggesting they were separate from the ER. The temperature shift had little effect on the distribution of 2C, which remained in perinuclear clusters (panels D and G). Figure 7E shows that FMDV 2C did not prevent movement of the G protein to the Golgi apparatus at 30 min (panel E) or to the cell surface after 3 h (panel I).

Finally, the same type of experiment was also performed for FMDV 2BC and is shown in Fig. 8. The 2BC protein produced punctate and reticular structures (panel A) reminiscent of the modified ER seen in Fig. 5I. In these cells, the G protein was

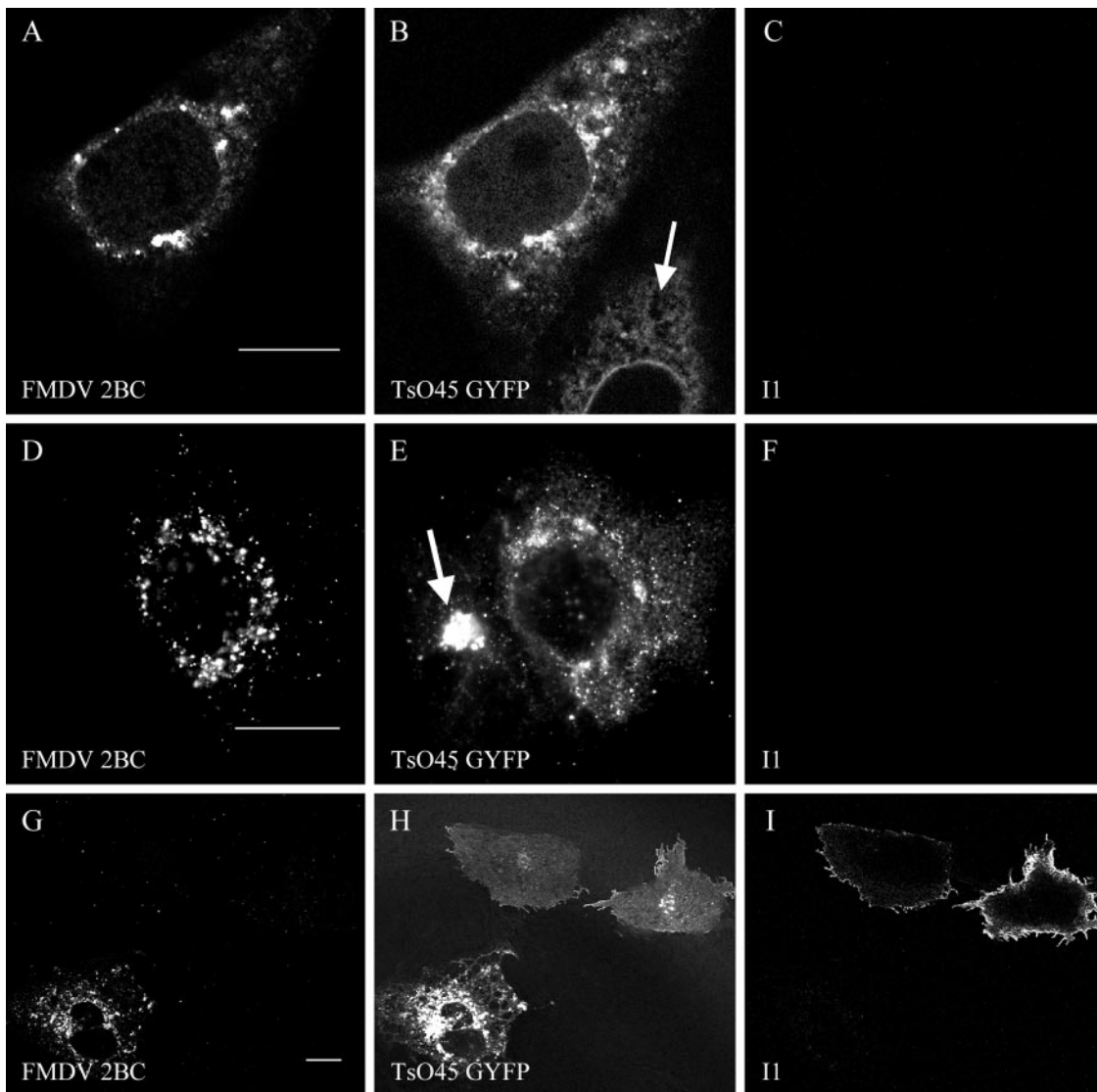


FIG. 8. FMDV 2BC blocks transport of VSV TsO45 GYFP protein to the cell surface. Vero cells were transiently cotransfected with TsO45 GYFP and FMDV 2BC and incubated for 48 h at 40°C (A to C). Some cells were also incubated for a further 30 min (D to F) or 3 h (G to I) at 32°C. All cells were fixed with 4% paraformaldehyde, and surface expression of the G protein was detected by adding an antibody (I1), recognizing the ectodomain of the G protein, prior to permeabilization (panels C, F, and I). Cells were then permeabilized, and 2BC was detected using antibody 3F7 (panels A, D and G). Intracellular TsO45 GYFP was visualized directly using the signal from YFP (panels B, E, and H). Primary antibodies were visualized with appropriate goat antibodies conjugated to Alexa-568 (panels A, D, and G) or Alexa-633 (panels C, F, and I). Bars, 10 μm. Arrows indicate cells transfected with TsO45 GYFP only and show the reticular pattern of the G protein in cells at 40°C (panel B) and the Golgi appearance of the G protein after moving the cells to 32°C (panel E) for 30 min.

also located in these modified structures, whereas in cells expressing the G protein alone (Fig. 8B), the G protein lacked punctate staining and was located in a reticular structure. When the cells were incubated for 30 min at 32°C, the 2BC protein was found in vesicular structures throughout the cytoplasm (panel D). Figure 8E shows the G protein in two cells, one of which is positive for 2BC staining (panel D). In the cell lacking 2BC (panel E, arrow), the G protein had concentrated within the Golgi apparatus; however, in the neighboring cell, expressing 2BC, the G protein failed to move to the Golgi apparatus and remained in vesicular structures scattered through the cytoplasm. Figure 8G to I show cells observed at 3 h after the temperature shift. Surface staining for the G

protein was now evident for cells lacking 2BC expression, but there was no surface staining in cells containing 2BC (panel I). Interestingly, there was no Golgi distribution for the G protein in those cells that also expressed FMDV 2BC and it remained in reticular and vesicular structures within the cytoplasm (panel H). The results indicated that FMDV 2BC causes intracellular retention of the G protein.

The intracellular reticular-punctate structures containing the TsO45 GYFP protein in FMDV 2BC-transfected cells were investigated further by using a triple transfection to locate the ER with DsRed2-ER as a marker. Cells transfected with plasmids expressing FMDV 2BC, DsRed2-ER, and TsO45 GYFP were maintained at 40°C for 48 h and then shifted to

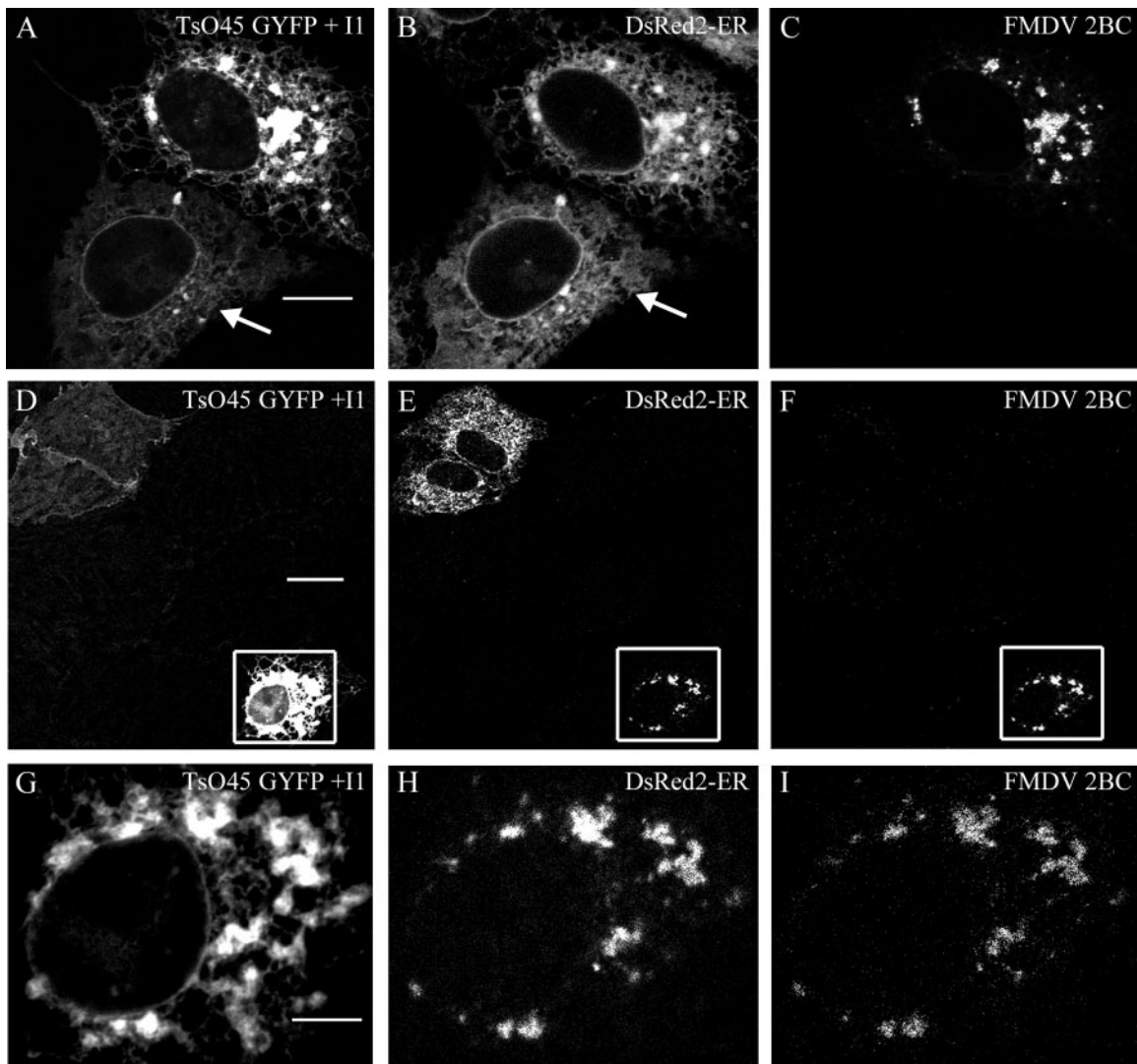


FIG. 9. VSV TsO45 GYFP cellular location in FMDV 2BC-transfected cells. (A to C) Vero cells were transiently cotransfected with vectors expressing TsO45 GYFP, DsRed2-ER, and FMDV 2BC proteins and incubated for 48 h at 40°C. (D to I) Some cells were also incubated for a further 3 h at 32°C. Surface expression of TsO45 GYFP protein was determined by immunofluorescence analysis of fixed, but not permeabilized, cells by using the antibody I1, specific for the ectodomain of the G protein (panels A, D, and G). Panels A, D, and G also show the internal location of TsO45 GYFP detected from the fluorescence of the YFP in transfected cells. Panels B, E, and H show the location of DsRed2-ER, a marker for the ER, detected from the DsRed2 fluorescence. Following I1 staining, cells were permeabilized and 2BC was detected using antibody DM12 (C, F, and I). Primary antibodies were visualized with appropriate goat antibodies conjugated to Alexa-488 (panels A, D, and G) or Alexa-633 (panels C, F, and I). Bars, 8 μ m (panel A), 20 μ m (panel D), and 4 μ m (panel G). Arrows indicate reticular patterns of the G protein and the ER marker.

32°C for 3 h. Cell surface G protein was analyzed as described above. Figure 9A to C show cells expressing TsO45 GYFP, DsRed2-ER, and FMDV 2BC grown at 40°C for 48 h. In cells expressing TsO45 GYFP and DsRed2-ER, both probes were collocated in a reticular structure (panels A and B). However, in cells also expressing the FMDV 2BC protein, the ER signal from DsRed2-ER was both punctate and reticular. It was apparent that the FMDV 2BC protein and the majority of the G protein (panels A to C) were located in these structures. The cells were then incubated for a further 3 h at 32°C. Panels D and E show that in cells that did not express FMDV 2BC, the G protein reached the surfaces of cells expressing DsRed2-ER

and DsRed2-ER remained located in a reticular network indicative of ER. The expression of DsRed2-ER did not therefore affect the transport of the G protein to the cell surface. The G protein was absent from the surfaces of cells expressing both DsRed2-ER and FMDV 2BC (Fig. 9D to F, insets). In these cells, the TsO45 GYFP was clearly seen retained within the cell, and at higher magnification, the G protein appeared in reticular structures associated with enlarged punctate structures (panel G). It was noticeable that the ER marker collocated with the G protein in punctate structures (panel H) positive for 2BC (panel I). These results suggest that 2BC modifies the ER into punctate structures which trap the TsO45 GYFP.

DISCUSSION

This study has investigated the effects of individual FMDV proteins 2B, 2C, 2BC, and 3A on the secretory pathway. All four proteins were associated with cellular membranes, and consistent with previous work, the FMDV 3A protein was found associated with the ER (32). FMDV 2B was located in structures closely associated with the ER, and at high levels of expression, the 2B protein caused rearrangement of the ER into a honeycomb of membranes close to the nucleus (results not shown). The exact nature of these structures is unclear. However, they may be related to organized smooth ER that can form in response to the overexpression of ER-localized proteins (42). The FMDV 2C protein showed some ER localization, but the majority of the protein was located in punctate structures formed within the Golgi apparatus. Surprisingly, when FMDV 2BC was expressed alone in cells, the immunofluorescence signal did not resemble either the ER-associated distribution of 2B or the Golgi location of 2C. Instead, 2BC was located in small punctate structures scattered throughout the cytoplasm and also to large punctate structures located around the nuclei. Interestingly, 2BC caused redistribution of ERp57 into brightly staining structures that also distributed around the nuclei, suggesting that 2BC could modify the ER.

The effects of the 3A, 2B, 2C, and 2BC proteins of FMDV on the function of the secretory pathway were analyzed by following the movement of the TsO45 mutant of the VSV G protein from the ER to the cell surface. Surprisingly, even though FMDV 3A, 2B, and 2C were located in membranes of the early secretory pathway, they did not block transport of the TsO45 GYFP protein from the ER to the Golgi apparatus or to the cell surface. It is not possible from our assay to show that 3A, 2B, and 2C did not slow the movement of the G protein from the ER to the Golgi apparatus and to the cell surface. Our study does, however, clearly show that following 30 min at the permissive temperature, 3A, 2B, and 2C had no obvious effect on movement of the G protein from the ER to the Golgi apparatus. In contrast, in the presence of FMDV 2BC, the TsO45 GYFP protein failed to reach the Golgi apparatus or surfaces of cells but localized with 2BC inside the cell. Triple-staining experiments showed that 2BC causes retention of the G protein in a modified ER compartment and that this retention lasts at least 3 h. The effect of FMDV 2BC on trafficking of the TsO45 GYFP protein was observed in about 200 cells at different levels of expression, and in each case, the expression of 2BC appeared to result in the retention of TsO45 GYFP within an intracellular vesicular compartment. The exact nature of these 2BC-positive structures containing the retained G protein and ER markers is not known but worthy of further investigation. Interestingly, in cells infected with PV or transfected with PV 2BC, the 2BC protein localizes to ER exit sites and sec13-positive vesicles (37). Sec13 is a component of the COPII complex which is involved in anterograde (ER-to-Golgi) vesicle formation and budding (4). In our studies, we were unable to colocalize sec13 with 2BC or the structures in which the TsO45 GYFP appears to accumulate (data not shown). The TsO45 GYFP does not therefore appear to accumulate at ER exit sites.

This study shows that FMDV differs from PV in the ability of nonstructural proteins to modulate the secretory pathway.

Evidence that different picornaviruses may utilize the secretory pathway in different ways has also been provided by previous studies (20, 23) in which it was demonstrated that three genera of the *Picornaviridae* show different sensitivities to BFA. This agent prevents Arf1-dependent recruitment of COP1 coats onto the Golgi apparatus, and the differential sensitivity to the drug suggests that different viruses have different requirements for COP1 coats during the formation of membrane vesicles utilized for replication. This is supported by the observation that COP1 is found associated with the replication complexes formed by BFA-sensitive viruses (parechovirus VI, echovirus 11) but not those resistant to the drug (encephalomyocarditis virus [EMCV]) (20). FMDV is also insensitive to BFA (30), so given the results from the present study, it will be interesting to see if other BFA-resistant viruses use 2BC rather than 3A to block ER-to-Golgi transport.

The PV 3A protein induces swelling of ER cisternae and a consequent block in the movement of proteins from the ER to the Golgi apparatus. In our study, the FMDV 3A protein also bound to the ER, but from immunofluorescence studies, it did not prevent the trafficking of the TsO45 GYFP protein to the cell surface. An explanation for this may lie in a comparison of the sequences of PV and FMDV 3A proteins. The PV 3A protein is 85 amino acids in length, while the FMDV protein is larger, with an extra 50 amino acids at the C terminus. Both proteins have hydrophobic domains that would explain their membrane association, but the N and C termini are very different. Interestingly, mutations near the N terminus of PV 3A reduce its ability to block ER-to-Golgi transport. This is most apparent from the insertion of a single serine residue between threonine 15 and serine 16 which produces a temperature-sensitive mutant unable to block secretion at 37°C (14). This N-terminal region also contains a series of proline residues conserved amongst the rhino- and enteroviruses but absent from the aphthoviruses (FMDV) and cardiociruses (EMCV). The loss of this region from FMDV may explain the lack of effect of the protein on ER-to-Golgi transport.

In mammalian cells, the PV 2B and 2BC proteins also slow movement of proteins to the cell surface (15). Since PV 2C does not block secretion when expressed alone, it is generally assumed that 2B is the active component of 2BC. Interestingly, the PV 2B protein does not block movement from the ER to the Golgi apparatus but rather arrests protein traffic in the Golgi apparatus. In our experiments, there was no intracellular arrest of traffic in cells expressing FMDV 2B. In a few cases, in cells expressing high levels of FMDV 2C, the G protein appeared to be retained in the cell, where it colocalized with 2C. However, this was seen in as few as 2% of cells examined. Observations from this study also point to differences in the types of membrane rearrangement induced by nonstructural proteins from different genera of picornaviruses. PV 2BC expressed alone in cells produces a punctate cytoplasmic staining which colocalizes with domains of the ER enriched for COP11 proteins, suggesting location to ER exit sites (37). In our experiments, FMDV 2BC also produced a punctate staining in the cytoplasm, but we were unable to colocalize these structures with proteins of the COP11 complex (data not shown). We also observed remodeling of the ER into large vesicular structures close to the nuclei in cells expressing FMDV 2BC. For PV, it is the 3A protein that remodels the ER by causing

swelling of ER cisternae, whereas the PV 2BC protein induces vesicle formation and PV 2C induces extensive tubular structures in the rough ER lumen (10, 43). The high level of sequence similarity in 3A seen between the rhinoviruses and other enteroviruses suggests that the 3A protein expressed by each of these viruses will also block membrane traffic, whereas the lower sequence similarity observed for 3A encoded by hepatitis A virus, Theiler's virus, and EMCV raises the possibility that they will behave differently and perhaps more like FMDV. Studies of hepatitis A virus-infected cells, using electron microscopy, showed that the 2BC protein modifies the ER into tight crystalloid structures (45). It may be that the hepatitis A 2BC protein also disrupts host membrane protein trafficking. Recent studies have investigated the ability of hepatitis C virus nonstructural proteins to induce membrane rearrangements and block the secretory pathway (24). Both the hepatitis C virus NS4B protein and its precursor NS4A/B expressed alone in cells produced a membranous web thought to be derived from the ER (17). Interestingly, only the precursor NS4A/B blocked ER-to-Golgi transport (24). This is analogous to our results with FMDV where only the precursor 2BC, but not the individual products (2B or 2C), is able to block the secretory pathway.

The observation that FMDV 2BC inhibits the delivery of membrane proteins to the cell surface raises the possibility that, as seen for PV 3A (11, 13–15, 31), the 2BC protein of FMDV may also be able to modulate the recognition of infected cells by the immune system. This could include a block in the secretion of interferons and proinflammatory cytokines or the inhibition of cell surface MHC class 1 expression (38) and antigen presentation. Such effects could contribute to the development of persistent infections that are frequently seen in ruminants following an acute FMDV infection. This study should therefore stimulate further investigation of the effects of FMDV 2BC on cytokine secretion and antigen presentation and the role the protein may play during the development of persistent FMDV infections in ruminants.

ACKNOWLEDGMENTS

We thank J. Lippincott-Schwartz for the kind gift of the plasmid TsO45 GCFP. We also thank E. Brocci for the FMDV antibodies 3F7 and 2C2 and D. Lyles for the I1 antibody against the ectodomain of VSV G. Finally, thanks to Steven Archibald for technical help with graphics.

This work was supported by BBSRC grants 49/C07867, 49/C14570, and 201/S14654 to Graham J. Belsham, Thomas Wileman, and Martin D. Ryan and the BBSRC bioimaging initiative 201/S11230.

REFERENCES

- Aldabe, R., A. Barco, and L. Carrasco. 1996. Membrane permeabilization by poliovirus proteins 2B and 2BC. *J. Biol. Chem.* **271**:23134–23137.
- Alexandersen, S., Z. Zhang, and A. I. Donaldson. 2002. Aspects of the persistence of foot-and-mouth disease virus in animals—the carrier problem. *Microbes Infect.* **4**:1099–1110.
- Barco, A., and L. Carrasco. 1998. Identification of regions of poliovirus 2BC protein that are involved in cytotoxicity. *J. Virol.* **72**:3560–3570.
- Barlowe, C., L. Orci, T. Yeung, M. Hosobuchi, S. Hamamoto, N. Salama, M. F. Rexach, M. Ravazzola, M. Amherdt, and R. Schekman. 1994. COPII: a membrane coat formed by Sec proteins that drive vesicle budding from the endoplasmic reticulum. *Cell* **77**:895–907.
- Bergmann, J. E. 1989. Using temperature-sensitive mutants of VSV to study membrane protein biogenesis. *Methods Cell Biol.* **32**:85–110.
- Bienz, K., D. Egger, and L. Pasamontes. 1987. Association of polioviral proteins of the P2 genomic region with the viral replication complex and virus-induced membrane synthesis as visualized by electron microscopic immunocytochemistry and autoradiography. *Virology* **160**:220–226.
- Bienz, K., D. Egger, Y. Rasser, and W. Bossart. 1983. Intracellular distribution of poliovirus proteins and the induction of virus-specific cytoplasmic structures. *Virology* **131**:39–48.
- Biron, C. A. 2001. Interferons alpha and beta as immune regulators—a new look. *Immunity* **14**:661–664.
- Biron, C. A. 1998. Role of early cytokines, including alpha and beta interferons (IFN-alpha/beta), in innate and adaptive immune responses to viral infections. *Semin. Immunol.* **10**:383–390.
- Cho, M. W., N. Teterina, D. Egger, K. Bienz, and E. Ehrenfeld. 1994. Membrane rearrangement and vesicle induction by recombinant poliovirus 2C and 2BC in human cells. *Virology* **202**:129–145.
- Deitz, S. B., D. A. Dodd, S. Cooper, P. Parham, and K. Kirkegaard. 2000. MHC I-dependent antigen presentation is inhibited by poliovirus protein 3A. *Proc. Natl. Acad. Sci. USA* **97**:13790–13795.
- de Silva, A. M., W. E. Balch, and A. Helenius. 1990. Quality control in the endoplasmic reticulum: folding and misfolding of vesicular stomatitis virus G protein in cells and in vitro. *J. Cell Biol.* **111**:857–866.
- Dodd, D. A., T. H. Giddings, Jr., and K. Kirkegaard. 2001. Poliovirus 3A protein limits interleukin-6 (IL-6), IL-8, and beta interferon secretion during viral infection. *J. Virol.* **75**:8158–8165.
- Doedens, J. R., T. H. Giddings, Jr., and K. Kirkegaard. 1997. Inhibition of endoplasmic reticulum-to-Golgi traffic by poliovirus protein 3A: genetic and ultrastructural analysis. *J. Virol.* **71**:9054–9064.
- Doedens, J. R., and K. Kirkegaard. 1995. Inhibition of cellular protein secretion by poliovirus proteins 2B and 3A. *EMBO J.* **14**:894–907.
- Egger, D., N. Teterina, E. Ehrenfeld, and K. Bienz. 2000. Formation of the poliovirus replication complex requires coupled viral translation, vesicle production, and viral RNA synthesis. *J. Virol.* **74**:6570–6580.
- Egger, D., B. Wölk, R. Gosert, L. Bianchi, H. E. Blum, D. Moradpour, and K. Bienz. 2002. Expression of hepatitis C virus proteins induces distinct membrane alterations including a candidate viral replication complex. *J. Virol.* **76**:5974–5984.
- Gallione, C. J., and J. K. Rose. 1985. A single amino acid substitution in a hydrophobic domain causes temperature-sensitive cell-surface transport of a mutant viral glycoprotein. *J. Virol.* **54**:374–382.
- Garcia-Mata, R., Z. Bebok, E. J. Sorscher, and E. S. Sztul. 1999. Characterization and dynamics of aggresome formation by a cytosolic GFP-chimera. *J. Cell Biol.* **146**:1239–1254.
- Gazina, E. V., J. M. Mackenzie, R. J. Gorrell, and D. A. Anderson. 2002. Differential requirements for COPI coats in formation of replication complexes among three genera of *Picornaviridae*. *J. Virol.* **76**:11113–11122.
- Hammond, C., and A. Helenius. 1994. Quality control in the secretory pathway: retention of a misfolded viral membrane glycoprotein involves cycling between the ER, intermediate compartment, and Golgi apparatus. *J. Cell Biol.* **126**:41–52.
- Heemels, M. T., and H. Ploegh. 1995. Generation, translocation, and presentation of MHC class I-restricted peptides. *Annu. Rev. Biochem.* **64**:463–491.
- Iruzun, A., L. Perez, and L. Carrasco. 1992. Involvement of membrane traffic in the replication of poliovirus genomes: effects of brefeldin A. *Virology* **191**:166–175.
- Konan, K. V., T. H. Giddings, Jr., M. Ikeda, K. Li, S. M. Lemon, and K. Kirkegaard. 2003. Nonstructural protein precursor NS4A/B from hepatitis C virus alters function and ultrastructure of host secretory apparatus. *J. Virol.* **77**:7843–7855.
- Kopp, E. B., and S. Ghosh. 1995. NF-kappa B and rel proteins in innate immunity. *Adv. Immunol.* **58**:1–27.
- Kreis, T. E., and H. F. Lodish. 1986. Oligomerization is essential for transport of vesicular stomatitis viral glycoprotein to the cell surface. *Cell* **46**:929–937.
- Lefrancios, L., and D. S. Lyles. 1982. The interaction of antibody with the major surface glycoprotein of vesicular stomatitis virus. I. Analysis of neutralizing epitopes with monoclonal antibodies. *Virology* **121**:157–167.
- Maynell, L. A., K. Kirkegaard, and M. W. Klymkowsky. 1992. Inhibition of poliovirus RNA synthesis by brefeldin A. *J. Virol.* **66**:1985–1994.
- Mezzacasa, A., and A. Helenius. 2002. The transitional ER defines a boundary for quality control in the secretion of tsO45 VSV glycoprotein. *Traffic* **3**:833–849.
- Monaghan, P., H. Cook, T. Jackson, M. Ryan, and T. Wileman. 2004. The ultrastructure of the developing replication site in foot-and-mouth disease virus-infected BHK-38 cells. *J. Gen. Virol.* **85**:933–946.
- Neznanov, N., A. Kondratova, K. M. Chumakov, B. Angres, B. Zhumabayeva, V. I. Agol, and A. V. Gudkov. 2001. Poliovirus protein 3A inhibits tumor necrosis factor (TNF)-induced apoptosis by eliminating the TNF receptor from the cell surface. *J. Virol.* **75**:10409–10420.
- O'Donnell, V. K., J. M. Pacheco, T. M. Henry, and P. W. Mason. 2001. Subcellular distribution of the foot-and-mouth disease virus 3A protein in cells infected with viruses encoding wild-type and bovine-attenuated forms of 3A. *Virology* **287**:151–162.
- Palade, G. 1975. Intracellular aspects of the process of protein synthesis. *Science* **189**:347–358.
- Presley, J. F., N. B. Cole, T. A. Schroer, K. Hirschberg, K. J. Zaal, and J.

- Lippincott-Schwartz.** 1997. ER-to-Golgi transport visualized in living cells. *Nature* **389**:81–85.
35. **Rothman, J. E., and F. T. Wieland.** 1996. Protein sorting by transport vesicles. *Science* **272**:227–234.
36. **Rouiller, I., S. M. Brookes, A. D. Hyatt, M. Windsor, and T. Wileman.** 1998. African swine fever virus is wrapped by the endoplasmic reticulum. *J. Virol.* **72**:2373–2387.
37. **Rust, R. C., L. Landmann, R. Gosert, B. L. Tang, W. Hong, H.-P. Hauri, D. Egger, and K. Bienz.** 2001. Cellular COPII proteins are involved in production of the vesicles that form the poliovirus replication complex. *J. Virol.* **75**:9808–9818.
38. **Sanz-Parra, A., F. Sobrino, and V. Ley.** 1998. Infection with foot-and-mouth disease virus results in a rapid reduction of MHC class I surface expression. *J. Gen. Virol.* **79**:433–436.
39. **Schekman, R., and L. Orci.** 1996. Coat proteins and vesicle budding. *Science* **271**:1526–1533.
40. **Schlegel, A., T. H. Giddings, Jr., M. S. Ladinsky, and K. Kirkegaard.** 1996. Cellular origin and ultrastructure of membranes induced during poliovirus infection. *J. Virol.* **70**:6576–6588.
41. **Schuler, G. D., S. F. Altschul, and D. J. Lipman.** 1991. A workbench for multiple alignment construction and analysis. *Proteins* **9**:180–190.
42. **Snapp, E. L., R. S. Hegde, M. Francolini, F. Lombardo, S. Colombo, E. Pedrazzini, N. Borgese, and J. Lippincott-Schwartz.** 2003. Formation of stacked ER cisternae by low affinity protein interactions. *J. Cell Biol.* **163**:257–269.
43. **Suhy, D. A., T. H. Giddings, Jr., and K. Kirkegaard.** 2000. Remodeling the endoplasmic reticulum by poliovirus infection and by individual viral proteins: an autophagy-like origin for virus-induced vesicles. *J. Virol.* **74**:8953–8965.
44. **Takegami, T., B. L. Semler, C. W. Anderson, and E. Wimmer.** 1983. Membrane fractions active in poliovirus RNA replication contain VPg precursor polypeptides. *Virology* **128**:33–47.
45. **Teterina, N. L., K. Bienz, D. Egger, A. E. Gorbalenya, and E. Ehrenfeld.** 1997. Induction of intracellular membrane rearrangements by HAV proteins 2C and 2BC. *Virology* **237**:66–77.
46. **Teterina, N. L., A. E. Gorbalenya, D. Egger, K. Bienz, and E. Ehrenfeld.** 1997. Poliovirus 2C protein determinants of membrane binding and rearrangements in mammalian cells. *J. Virol.* **71**:8962–8972.
47. **Troxler, M., D. Egger, T. Pfister, and K. Bienz.** 1992. Intracellular localization of poliovirus RNA by in situ hybridization at the ultrastructural level using single-stranded riboprobes. *Virology* **191**:687–697.
48. **van Kuppeveld, F. J., W. J. Melchers, K. Kirkegaard, and J. R. Doedens.** 1997. Structure-function analysis of coxsackie B3 virus protein 2B. *Virology* **227**:111–118.